Journal of Hazardous Materials 422 (2022) 126864

Contents lists available at ScienceDirect

Journal of Hazardous Materials

journal homepage: www.elsevier.com/locate/jhazmat

Research Paper

Development of nanoporous textile sludge based adsorbent for the dye removal from industrial textile effluent

Ninad Oke [1], S. Mohan [*]

Indian Institute of Technology Madras, Environmental and Water Resources Engineering Division, Department of Civil Engineering, Chennai, Tamil Nadu 600036, India

ARTICLE INFO

Editor: Dr. H. Artuto

Keywords:
Textile sludge
Adsorption
Dye removal
Column studies
Adsorbent reuse

ABSTRACT

The development of a novel textile sludge based activated carbon (TSBAC) adsorbent and its performance for the treatment of textile dyeing effluent, have been explained in this paper. TSBAC was prepared by the thermal treatment of textile effluent treatment sludge followed by the chemical activation using phosphoric acid. Characterization of TSBAC resulted in enhanced specific surface area (123.65 m^2/g) along with the presence of active surface functional groups including −OH, −COOH, −C═O. TSBAC showed superior adsorption capacity for methylene blue (123.6 mg/g), reactive red 198 (101.4 mg/g), and reactive yellow 145 (96.8 mg/g) individually, and from the synthetic textile effluent (106 mg/g). The pseudo-second order model and Langmuir isotherm model were found to be fitted well with batch experimental data. The results of the continuous column studies showed that adsorption capacity for methylene blue, reactive red 198, reactive yellow 145 are 101.8 mg/g, 76.6 mg/g, and 75.1 mg/g respectively, and the synthetic textile effluent resulted in an adsorption capacity value of 79.1 mg/g. The reuse potential of TSBAC was proved by effective dye removal up to six reuse cycles. The leachability studies proved that the used adsorbent could be safely disposed of without any harmful effect to the environment.

1. Introduction

The textile dyeing industry is well-known as one of the most complex manufacturing industries with potentially high water, energy, and chemical resource consumption as well as generation of large quantity of hazardous effluent (Paździor et al., 2019). The presence of hydrolyzed dyes in the textile effluent poses major risks to the aquatic ecosystem including reduced transparency interfering photosynthesis, higher organic load leading to reduced dissolved oxygen levels, and toxicity to aquatic flora and fauna (Choudhary et al., 2020; Varjani et al., 2020). Partially treated dye compounds are reported to be eye and skin irritants and known to cause mutagenic and carcinogenic effects on human body (Sonai et al., 2016; Yadav et al., 2021).

The azo type of dyes widely used for textile dyeing are found to be resistant to physical separation methods, aerobic degradation, and oxidizing agents (Wong et al., 2018). The efficient dye removal from industrial textile effluent is required due to the possible bio-accumulation and biomagnification of the dye compounds in the food chain (Jiang et al., 2019). Most of the dye compounds are recalcitrant in nature and tend to accumulate in the biomass as they cannot be degraded by the organisms. Thus, in most of the biological treatment systems for textile effluent treatment, dye molecules are found in the sludge without any degradation. The most common mechanism involved in the interaction between dye molecules and cell biomass is biosorption (Lellis et al., 2019). Khan and Kumar (2016) have suggested formation of RNA-azo dye complex leading to possible bioaccumulation of dyes. Polyaromatic dye compounds with strong electron withdrawal groups like azo group, −Cl tend to be bioaccumulated as the biological system cannot degrade these complex dye molecules. When directly discharged to the environment, dyes persist in environment and can traverse through the entire food chain. Once dye molecules enter in the food chain, their concentration can reach harmful levels based on the increasing consumption rate at higher levels in the food chain. Among various treatment methods, adsorption is widely used considering its low capital investment, simple operation, targeted pollutant removal, and no generation of reaction intermediates (Liu et al., 2020). The chemically activated low-cost waste materials like *Jatropha* seeds, cashew nut shells, sugarcane bagasse have been used as activated carbon

* Corresponding author.
E-mail addresses: ce16d006@smail.iitm.ac.in (N. Oke), smohan@iitm.ac.in (S. Mohan).
[1] ORCID: 0000-0001-9786-3846

https://doi.org/10.1016/j.jhazmat.2021.126864
Received 24 May 2021; Received in revised form 4 August 2021; Accepted 6 August 2021
Available online 8 August 2021

for the adsorptive removal of the dyes (Saheed et al., 2017; Spagnoli et al., 2017; Zheng et al., 2020).

With the increasing product demand from textile manufacturing sector, the management of hazardous sludge arising from textile effluent treatment has become a major concern for minimizing the environmental impacts of this ever-growing sector. It is estimated that textile effluent plants in Bangladesh alone generated 36 million tons of textile sludge in 2012, which is expected to increase to 80 million tons by 2021 (Haque, 2020). Textile sludge generation rate was found to be nearly 1.14 kg per m^3 of textile effluent being treated (Rahman et al., 2017). The textile manufacturing cluster at Tiruppur in Tamil Nadu state, India having nearly 800 manufacturing units generates nearly 200 ton textile sludge per day (Begum et al., 2013). Though, various researchers have studied the use of stabilized textile sludge as a construction material, potential field-scale management solution remains a challenge (Zhan et al., 2020; Beshah et al., 2021). A study by Wong et al. (2018), reported that dye adsorption capacities of 11.98 mg/g and 13.27 mg/g for reactive black 5 and methylene blue, respectively by the textile effluent treatment sludge based adsorbent activated by H_2SO_4. The field-scale application potential of the adsorbent cannot be determined owing to the use of simple dye solutions for adsorption studies and lack of continuous column adsorption studies.

Various activating agents like $ZnCl_2$, H_2SO_4, and CH_3COOH are applied to enhance surface characteristics of the developed adsorbents (Vasques et al., 2009; Gupta and Garg, 2015). The chemical activation by applying phosphoric acid has been reported for the preparation of various low-cost adsorbents including rice husk (Mohan and Sreelakshmi, 2008), coffee grounds (Reffas et al., 2010), corn stalks (Tang et al., 2019), and banana peel (Oyekanmi et al., 2019).

Based on the reported studies on adsorptive removal of hydrolyzed dye compounds, certain functional groups in the dye structure are responsible for the adsorption of the dye molecule on the adsorbent surface. Various functional groups including sulphonic acid group and $-NH_2$ group are proved to be responsible for the dye adsorption (Haider et al., 2011; Wu et al., 2020).

Thus, reported research work aimed at developing a textile sludge based activated carbon for adsorptive removal of the complex hydrolyzed dye molecules. In the present research work preliminary studies were conducted using chemical activating agents like acetic acid, sulfuric acid, and phosphoric acid. Percentage dye removal from synthetic textile effluent was found to be about 69%, 81%, and 90% for the adsorbents activated using acetic acid, sulfuric acid, and phosphoric acid, respectively. Based on the higher dye removal efficiency achieved in the preliminary batch adsorption studies, phosphoric acid was selected for the chemical activation. Thus, the approach adopted in the study is to use the textile effluent treatment sludge with activation by phosphoric acid and to assess its performance in the dye removal from synthetic textile effluent. Also, the proposed technique solves both the problems of treatment of textile effluent as well as solving the textile sludge disposal problem, thus resulting in a win-win situation; both for treatment of effluent and the effective reuse of sludge.

The dye removal efficiency of the developed adsorbent (thermochemically treated textile sludge) was determined by batch adsorption studies. The use of only individual dye solution as the adsorbate solution may prove to be misleading for field-scale application of the adsorbent owing to the complexity of real textile effluent. Thus, dye removal efficiency of the developed adsorbent with synthetic textile effluent containing a mixture of dyes was also analyzed in the present study. Surface characterization was performed to study surface functional groups and surface morphology of the developed adsorbent.

For any developed adsorbent, the results of column adsorption studies are important to provide various operational parameters which are customizable for long term use and to ensure potential field-scale application (Basu et al., 2019). The fixed-bed continuous column adsorption studies were performed to understand the dynamic adsorption performance in a long-run. Breakthrough curves were also developed for all the adsorbate solutions at different bed depths (10, 20, and 30 cm) of the adsorbent beds. The possible dye adsorption mechanism for the developed adsorbent is also described. The leachability studies were conducted for spent adsorbent using toxicity characteristics leaching procedure (TCLP) and it was found that the used adsorbent has very low leachability, thus ensuring safe disposal of the same without any damage to environment.

2. Materials and methods

2.1. Adsorbent preparation

Textile sludge (TS) was collected from a textile industry in Erode, Tamil Nadu, India, with a production capacity of 3500 kg fabric per day. The industry produces nearly 750 m^3 per day of textile effluent along with nearly 160 kg textile sludge generation per day. The collected TS represented the sludge from both primary and secondary settling units.

The raw sludge sample was oven dried at 105 °C for 24 h to remove the moisture content. The oven-dried sludge was then crushed into powder form. The particles with the size range of 0.420 mm (sieve #40) to 0.105 mm (sieve #140) were selected for further processing. The thermal treatment of textile sludge was carried out in a muffle furnace (Everflow Scientific, India) at the temperature of 500 °C (Vasques et al., 2009; Sonai et al., 2016; Leal et al., 2018). During thermal treatment, inert atmosphere was maintained using nitrogen at 150 cm^3/min flow rate. With heating rate of 5 °C/min, the temperature of 500 °C was maintained for 1 h duration as weight of the solids was found to be constant after 1 h. For chemical activation, 10 g of textile sludge after thermal treatment, was added to 100 mL of 0.5 M phosphoric acid. The solids were kept submerged in the phosphoric acid overnight (nearly 12 h) to allow sufficient time for the surface activation. The solids were filtered out from the mixture and resulting product was washed with distilled water until wash water pH becomes constant. The adsorbent was then oven-dried at 105 °C for 12 h and stored in air-tight containers for further use.

2.2. Adsorbent characterization

A porosimeter (Micromeritics ASAP 2020, USA) was used to analyze the Brunauer-Emmett-Teller (BET) surface area, pore volume, and average pore size of the developed adsorbent using nitrogen adsorption/desorption isotherms. The scanning electron microscope (SEM) images of the developed adsorbent were obtained using FEI Quanta 200, Netherlands, high resolution scanning electron microscope to perform comparative study of the surface morphology of raw textile sludge and the developed adsorbent. The point of zero charge (pH_{PZC}) of the adsorbent was estimated by pH drift method (Kołodyńska et al., 2016) and surface functional groups were investigated by Fourier-transform infrared (FTIR) spectrum recorded from 400 to 4000 cm^{-1} (Perkin Elmer, Spectrum 100, Germany). The XPS spectra of TSBAC before and after adsorption was obtained using SEM/SAM+XPS analyzer provided by SPECS group, Germany. The CasaXPS software was used for deconvolution of XPS spectra. The water contact angle for textile sludge and TSBAC was determined using a goniometer system OCA15 + (Data physics, Germany). The measurements were taken using Milli-Q water at ambient temperature with a drop volume of 2 microliter.

2.3. Adsorbate solutions

Dye removal efficiency of the developed adsorbent was tested with three different dye compounds namely methylene blue (MB), reactive red 198 (RR 198), and reactive yellow 145 (RY 145). These dye compounds were selected as they represent the three basic colors used for making all other color shades. Various properties of the selected dye compounds are listed in Table 1. The molecular structures of different dye compounds used in this study are presented in the supplementary

Table 1
Properties of selected dye compounds.

Properties	MB	RR 198	RY 145
Chemical formula	$C_{16}H_{18}ClN_3S$	$C_{27}H_{18}ClN_7Na_4O_{16}S_5$	$C_{28}H_{20}ClN_9Na_4O_{16}S_5$
CAS number	61–73–4	145017–98–7	93050–80–7
Molecular weight	319.9	984.2	1026.3
UV absorption maxima (λ_{max})	664 nm	512 nm	415 nm
Type of dye	Cationic thiazine	Anionic reactive azo	Anionic reactive azo
Use	Used as a dye in silk, textile, paper, and cosmetics	Widely used for the dyeing of cellulose or cotton fabric	Used for cellulose fiber, polyester, and cotton dyeing

material.

It can be observed from Table 1 that the considered azo type of dye compounds are widely used for cellulose and polyester dyeing. Four different adsorbate solutions were used for the batch and continuous column adsorption studies, including three individual dye solutions along with the synthetic textile effluent. The synthetic textile effluent was prepared using above three dyes in equal proportion, NaCl, glucose, and starch as the effluent constituents. It was prepared to have similar wastewater quality parameters as the real textile effluent collected from the equalization tank of the textile manufacturing industry in Erode, Tamil Nadu, India. Various production stages in textile manufacturing along with the effluent generation data per 100 kg of the textile product manufactured is provided in the supplementary material. Characteristics of the real and synthetic textile effluent are presented in Table 2. Starch and glucose were added to adjust the chemical oxygen demand (COD) and biochemical oxygen demand (BOD) of the synthetic effluent. NaCl salt was used to achieve the required Total Dissolved Solids (TDS) concentration as it is widely used by the textile manufacturing units. pH of the samples was measured with a glass electrode attached to a microprocessor pH Stat/Analyzer (Polman, Model: LP-139S, India). pH of the adsorbate solutions was adjusted using 0.1 N H_2SO_4 and NaOH solutions. All the chemicals used in present study were of analytic grade.

2.4. Batch adsorption experiments

To perform batch adsorption studies, the developed adsorbent was mixed with 100 mL of the adsorbate solution at 150 rpm till the adsorption equilibrium was reached. The effect of initial pH (2−10), initial dye concentration (50–400 mg/L), and adsorbent dose (0.5–4 g/L) on the dye removal efficient was analyzed.

During the batch adsorption studies, 1.5 mL of sample was collected at 5, 10, 15, 30, 60, and 90 min reaction time and filtered through a filter membrane (0.2 μm) to remove solids. Three individual dye solutions prepared using methylene blue (MB), reactive red 198 (RR 198), and reactive yellow 145 (RY 145) were used to determine individual dye adsorption capacities. Synthetic textile effluent was used as the fourth adsorbate solution to determine dye adsorption capacity from synthetic textile effluent. The absorbance of the samples was measured between 200 nm and 800 nm using a UV Visible Spectrometer (UV-Vis Shimadzu 260, Japan) to determine the dye concentration. In case of individual dye solutions, calibration curve was developed for the dye compounds between dye concentration and UV absorbance at λ_{max} as given in Table 1. As the synthetic textile effluent consists of all the three dyes, calibration curve was developed between total dye concentration and area under the UV absorbance curve between 200 nm and 800 nm. The dye concentrations in the collected samples were determined using the developed calibration curves. The batch adsorption experiments were done in triplicate and the average values were used as the experimental data. The equations used to calculate quantity of adsorbed dye and percentage dye removal for batch adsorption studies are given in supplementary material. Equilibrium adsorption data obtained at different initial dye concentrations was fitted to various isotherm models. Various models including pseudo-first order, pseudo-second order, and intra-particle diffusion model were applied to understand adsorption kinetics.

Table 2
Characteristics of real and synthetic textile effluent.

Parameter	Real Textile Effluent	Synthetic Textile Effluent
pH	10.8	10.6
Conductivity (μS/cm)	8550 ± 150	7990 ± 200
COD (mg/L)	2809 ± 180	2754 ± 40
BOD_5 (mg/L)	620 ± 82	670 ± 128
Total Suspended Solids (mg/L)	3672 ± 120	3124 ± 90
Total Dissolved Solids (mg/L)	5728 ± 100	5244 ± 180
Absorbance at 436 nm	2.02	2.54
Absorbance at 525 nm	1.36	1.82
Absorbance at 620 nm	1.06	1.76

2.5. Continuous column adsorption experiments

The schematic diagram of experimental setup for fixed-bed continuous column adsorption studies is presented in Fig. 1. The glass column of internal diameter of 2.5 cm with a total height of 60 cm was used. A total of 24.8 g of the developed adsorbent was packed over glass wool leading to a bed height of 30 cm. Based on the past studies, flow rate of 20 mL/min was maintained using peristaltic pump (Mohan and Sreelakshmi, 2008). Continuous column studies were conducted for all the four adsorbate solutions specified in Section 2.3 at the initial dye concentration of 250 mg/L.

The breakthrough curves were obtained from columns of different bed heights (10, 20, 30 cm) by collecting samples at 15 min interval, and sample dye concentration was determined as described in Section 2.4. The continuous column adsorption experiments were done in triplicate and the average values were used for dynamic adsorption modeling. Various equations used in the present study to calculate dye adsorption capacity and percentage dye removal for continuous column adsorption studies are given in supplementary material. The breakthrough time and exhaustion time were considered as the time corresponding to when C_t/C_0 has a value of 0.1 and 0.9, respectively. The experimental data was fitted through a breakthrough curve and analyzed for its fit to various dynamic adsorption models.

2.6. Reuse of adsorbent

The reuse potential for TSBAC was analyzed by reusing the spent adsorbent from batch adsorption studies. The spent adsorbent was subjected to oven drying at 105 °C for 24 h before each reuse cycle. The possible reuse of spent adsorbent was evaluated by batch adsorption of the dyes in synthetic textile effluent at pH 3, initial dye concentration of 250 mg/L and 2 g/L of adsorbent dose for each reuse cycle. Percentage dye removal from the synthetic textile effluent was determined after each reuse cycle and the concentration of adsorbent was kept constant in subsequent reuse cycles. Reuse experiments were repeated three times and the average values of percentage dye removal were considered.

2.7. Leachability studies

The leaching potential of the adsorbed dyes from spent adsorbent

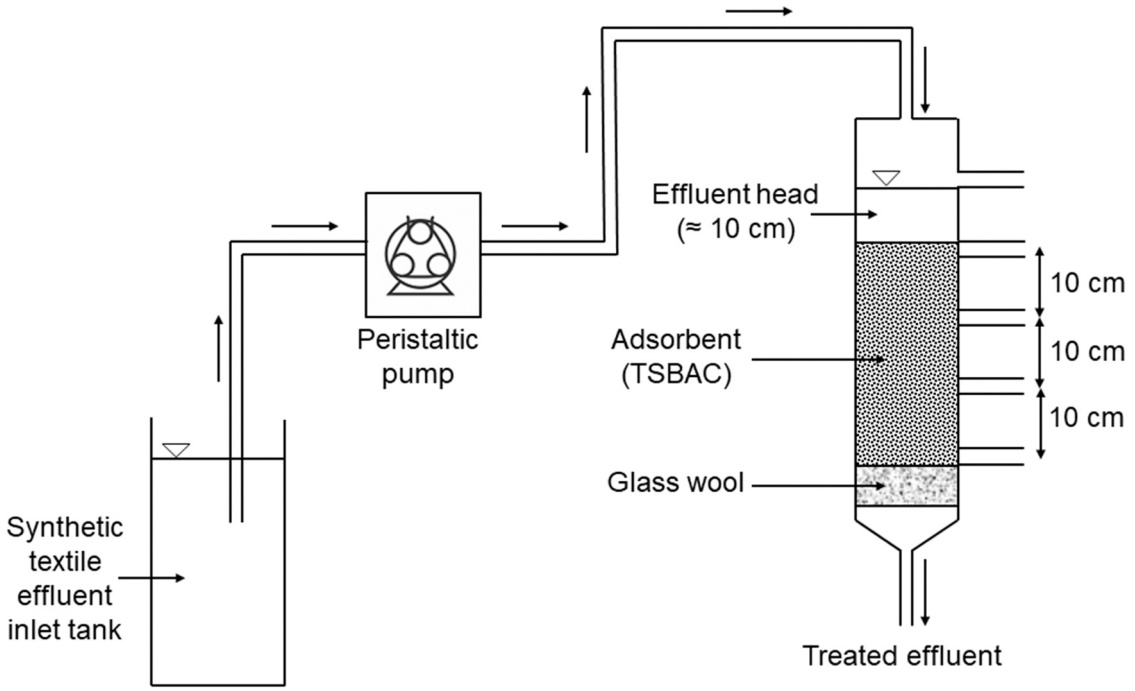

Fig. 1. Experimental setup for continuous column adsorption studies.

was determined by toxicity characteristics leaching procedure (TCLP) (U.S. EPA, 2012). First, batch adsorption experiments were performed using three separate adsorbate solutions made using methylene blue (MB), reactive red 198 (RR 198), and reactive yellow 145 (RY 145). The initial amount of adsorbed dye was determined by multiplying the amount of spent adsorbent used for TCLP test and experimentally determined adsorption capacity. The spent adsorbent was mixed with extraction solution at a liquid to solid ratio of 20. The extraction solution was prepared using 0.1 M acetic acid and 0.0643 M sodium hydroxide resulting in a pH of 4.93. The suspension was then mixed at 30 rpm for the duration of 18 h. The spent adsorbent was then filtered out and dye concentration in the solution was determined by the method described in Section 2.4. The dye concentration in extraction solution was multiplied by the volume of extraction solution to determine amount of dye released from spent TSBAC. The experiments were repeated three times and the average values were used to determine percentage dye released from the spent adsorbent.

3. Results and discussion

3.1. Characterization of adsorbent

The particle size of developed adsorbent was between 0.105 and 0.420 mm, which facilitated the complete removal of spent adsorbent after adsorption treatment by microfiltration. Various characteristics of the developed adsorbent (TSBAC) are presented in Table 3.

The thermo-chemical activation of TS imparted nanoporous surface morphology to the TSBAC as confirmed by the SEM images presented in Fig. 2. BET surface area of TSBAC (123.65 m^2/g) increased after the thermo-chemical activation of TS (84.33 m^2/g). Also, pore volume increased from 0.16 cm^3/g to 0.36 cm^3/g by phosphoric acid activation. Previous studies using textile sludge based adsorbents have reported BET surface area of 44 and 38.4 m^2/g (Sonai et al., 2016; Leal et al., 2018). The BET surface area of TSBAC was found to be nearly 200% more than the reported values. Average pore diameter of 0.144 nm indicates nanoporous nature of TSBAC. The increased BET surface area and pore volume result in enhanced dye adsorption and reduced diffusion resistance (Mahmoud et al., 2012).

Table 3
Characteristics of TSBAC adsorbent.

Parameter	TSBAC
Particle size (sieve size in mm)	0.105–0.420
pH_{PZC}	4.3
BET surface area (m^2/g)	123.65
Volume of pores (cm^3/g)	0.36
Average pore diameter (nm)	0.144

The hydrophilicity and hydrophobicity of TSBAC was measured using the water contact angle measurements. The water contact angle was found to be 79.5° ± 2° and 65° ± 2° for TS and TSBAC, respectively. The decrease in water contact angle and increase in hydrophilic nature can be attributed to the presence of hydroxyl groups on the surface of TSBAC (Liu et al., 2021; Lei et al., 2021a). Similar increase in the hydrophilicity due to the presence of hydroxyl groups on the material surface was reported by Lei et al. (2021b). The observed water contact values for the developed adsorbent were in line with the previously reported water contact angle values for natural material based activated carbon (Kusworo et al., 2018; Gopi et al., 2019).

The active surface functional groups on TSBAC were analyzed based on the FTIR spectrum as presented in Fig. 3. The wide band from 3200 to 3600 cm^{-1} corresponds to O−H stretching of the hydroxyl group along with N − H stretching of amine and amide groups (Saha et al., 2012; Xu et al., 2014; Cheng et al., 2019; Zheng et al., 2020). Various forms of oxygen in TS could have transformed into C−O bonds during the thermal treatment as presented by the peak at 1050 cm^{-1}. These C−O bonds are in fact responsible for the efficient adsorption.

The strong peak corresponding to wave number 1000 cm^{-1} in case of TSBAC could also be attributed to P − O−P and P═O stretching confirming successful activation by phosphoric acid (Tang et al., 2019). The peaks corresponding to aromatic C═C stretching (1409 cm^{-1}, 1458 cm^{-1}) and aliphatic −CH group (2920 cm^{-1}) disappeared after the activation of TS (Yao et al., 2020). As observed from the FTIR spectra of TS and TSBAC, various oxygen containing active surface functional groups like −OH, −COOH, and −C═O were introduced in TSBAC by the thermo-chemical treatment. The FTIR spectrum of TSBAC after dye adsorption presents reduction in the peaks corresponding to the active

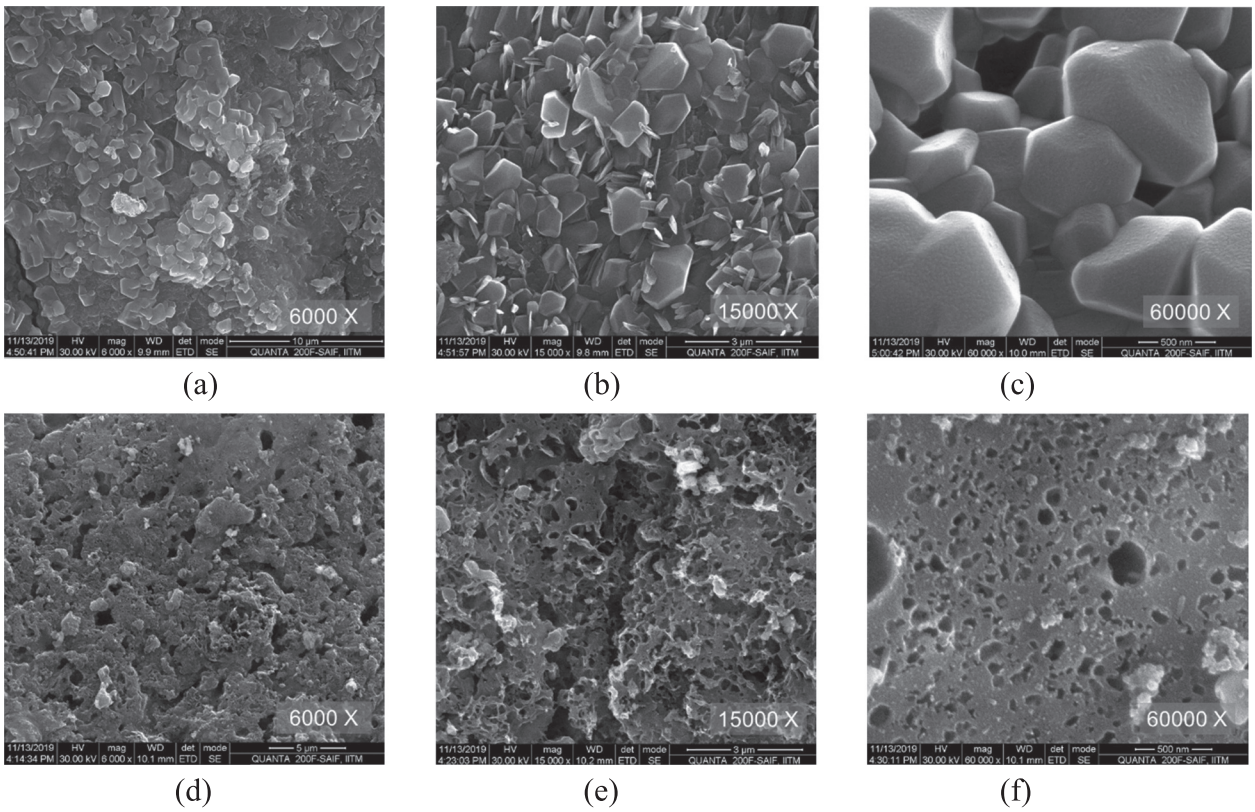

Fig. 2. SEM images of textile sludge (a-c), textile sludge based activated carbon (d-f).

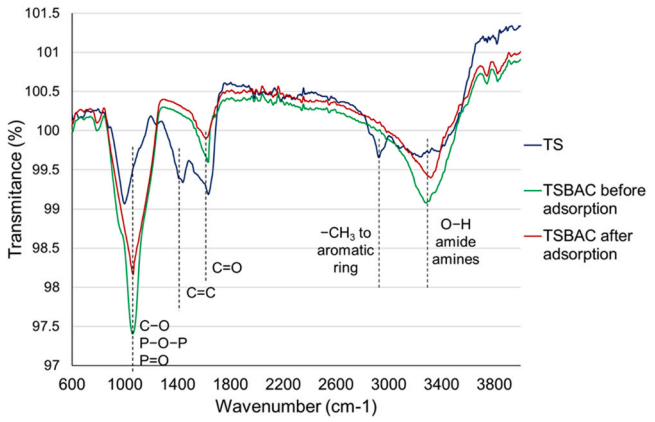

Fig. 3. FTIR spectra of TS and TSBAC before and after dye adsorption showing surface functional groups.

surface functional groups like −OH, C−O, and −C═O. This indicates the involvement of −OH, C−O, and −C═O as the binding sites for the hydrolyzed dye molecules.

3.2. Batch equilibrium studies

3.2.1. Effect of system parameters

The adsorption equilibrium for batch studies was considered to have attained after 90 min run time as no more significant increase in the percentage dye removal was observed for all considered adsorbate solutions. A control run was performed for 90 min, without addition of any adsorbent to ensure stability of the adsorbate solution. Thus, any reduction in UV absorbance during batch studies was attributed to the adsorptive dye removal.

The initial solution pH has a significant effect on the surface functionality of the developed adsorbent. The pH was varied from 2 to 10 while, adsorbent dose was kept as 2 g/L and the initial dye concentration was 50 mg/L. The pH_{PZC} value determines the adsorbent surface charge under various pH conditions (Sonai et al., 2016). The pH_{PZC} value of TSBAC was found to be 4.3. The optimum pH value of 3 was found for the dye adsorption of RR 198 (79.3%), RY 145 (76.0%), and synthetic textile effluent (90.2%) on TSBAC. A previously reported study by Venkataraghavan et al. (2020) also observed higher percentage dye removal at pH 3 in case of real textile effluent adsorption over activated carbon prepared using *Gracilaria edulis*. At pH < pH_{PZC} the TSBAC surface has positive charge, favoring the adsorption of anionic hydrolyzed RR 198 and RY 145. The optimum pH of 5 was obtained in case of MB (97.0%) adsorption on TSBAC. At pH > pH_{PZC} the TSBAC surface has negative charge, favoring the adsorption of cationic hydrolyzed MB. For the adsorption experiments conducted using individual dye solution of reactive red 198 (RR 198), reactive yellow 145 (RY 145), and synthetic textile effluent at the optimum pH of 3, slight increase in the pH was observed after adsorption with final pH of 3.6. This can be attributed to the uptake of H^+ ions by the TSBAC surface. In case of methylene blue (MB) adsorption conducted at the optimum pH of 5, slight reduction in the pH was observed after adsorption with final pH of 4.5.

The adsorbent dose was varied from 0.5 g to 4 g/L with the increment of 0.5 g/L to study the effect on dye adsorption. The initial dye concentration was 250 mg/L and optimum pH for respective adsorbate solutions was maintained. The percentage dye removal was found to increase up to 2 g/L and almost remains the same thereafter. The equilibrium between adsorbed dye molecules on TSBAC surface and dye molecules in the adsorbate solution was attained at an adsorbent dose of 2 g/L leading to no further increase in adsorption capacity despite availability of the adsorption sites at higher adsorbent doses (Mamaní et al., 2019). The adsorption efficiency of the developed adsorbent was found significantly higher as Patel and Vashi (2010) reported around 90% color removal from real textile effluent by activated charcoal at the

adsorbent dose of as high as 11 g/L.

3.2.2. Adsorption isotherm studies

The adsorption isotherms for the TSBAC related to the removal of considered dye compounds were developed by varying initial dye concentration from 50 to 400 mg/L, with the adsorbent dose of 2 g/L at the optimum pH for adsorption. Three adsorption isotherms including Langmuir, Freundlich, and Temkin were tested for fitting the experimental data. The Langmuir adsorption model represents monolayer adsorption on homogeneous adsorbent surfaces (Langmuir, 1916). The Freundlich adsorption model is an empirical model applicable to multilayer adsorption over a non-uniform adsorbent surface with selective adsorption sites (Freundlich, 1909). The Temkin adsorption model is widely used for heterogeneous adsorbent surface with uniform binding energy distribution (Temkin and Pyzhev, 1940). The Langmuir, Freundlich, and Temkin isotherm equations are provided in the supplementary material.

The adsorption isotherm plots for the considered adsorbate solutions are presented in Fig. 4. Various isotherm parameters for dye adsorption on TSBAC from the present study are presented in Table 4.

The R^2 values for Langmuir isotherm were higher than the R^2 values for Freundlich and Temkin isotherm for all the considered adsorbate solutions. The maximum adsorption capacities predicted by Langmuir isotherm model were in-line with the observed experimental adsorption capacities.

The adsorption capacity for MB was higher as compared to RR 198 and RY 145 owing to the lower molecular size of the hydrolyzed MB molecules (Wu et al., 2016). The separation factor (R_L) was calculated using Langmuir isotherm constant and initial dye concentration to ensure feasibility of the dye adsorption on TSBAC. Based on the R_L value, nature of the isotherm can be determined to be favorable ($0 < R_L < 1$), unfavorable ($R_L > 1$), linear ($R_L = 1$), and irreversible ($R_L = 0$).

The R_L value of less than 1 for all considered C_0 values and $0 < 1/n < 1$ for Freundlich isotherm fitting data indicates the dye adsorption on TSBAC was feasible. The plots presented in Fig. 4, show the characteristic L-shaped curve as per the classification developed by Giles et al. (1974). This confirms the suitability of Langmuir isotherm and indicates that the monolayer dye adsorption becomes difficult with increasing percentage of occupied active sites in the TSBAC surface.

3.2.3. Adsorption kinetics

It is important to predict the relationship between adsorption capacity and reaction time to understand the interactions of adsorbate solutions and TSBAC. The adsorption kinetics of considered model dyes on TSBAC was studied by applying pseudo-first order (Lagergren, 1898), pseudo-second order (Blanchard et al., 1984) and Weber-Morris intraparticle diffusion model (Weber and Morris, 1963). The adsorption kinetic parameters for MB, RR 198, RY 145, and the dyes in synthetic textile effluent are presented in Table 5. The equations of kinetic models used in the present study are given in the supplementary material.

The R^2 values for pseudo-first order model and intraparticle diffusion model were found to be lower than the R^2 values for pseudo-second order model in case of all the considered adsorbate solutions. The predicted adsorption capacities by the pseudo-second order model and experimental adsorption capacities were in good match. The results of kinetic studies suggest chemisorption was the rate-limiting step for the dye adsorption on the developed adsorbent TSBAC as postulated for the other adsorbent namely coal fly ash by Mohan and Gandhimathi (2009). The observation that q_t vs $t^{1/2}$ plot does not pass through origin suggests that the film diffusion determines rate of adsorption rather than

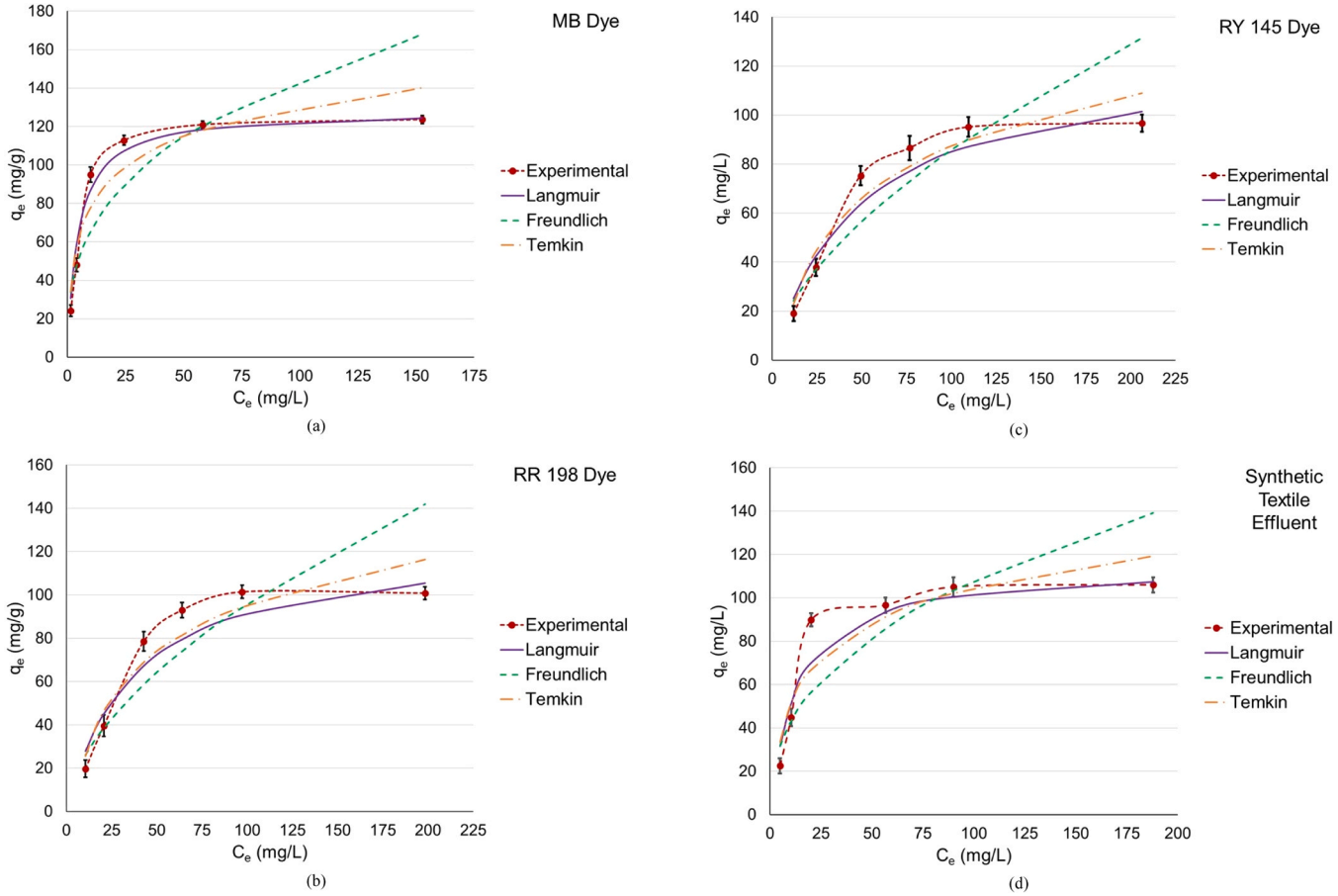

Fig. 4. Adsorption equilibrium data fit to various isotherm models for dye adsorption on TSBAC (a) MB (b) RR 198 (c) RY 145 (d) Synthetic Textile Effluent.

Table 4
Isotherm parameters for dye adsorption on TSBAC.

Adsorbate	$q_{e\ (exp.)}$ (mg/g)	Langmuir			Freundlich			Temkin		
		q_m (mg/g)	K_L (L/mg)	R^2	K_F (L/mg)	n	R^2	K_T (L/mg)	b_T (J/mol)	R^2
MB	123.6	128.20	0.21	0.99	29.22	2.87	0.81	2.96	108.82	0.89
RR 198	101.4	125.00	0.03	0.95	6.72	1.73	0.85	0.22	80.78	0.89
RY 145	96.8	125.00	0.02	0.95	5.48	1.67	0.86	0.17	82.24	0.92
Dyes in Synthetic Textile Effluent	106	114.94	0.08	0.98	16.80	2.47	0.78	0.85	106.01	0.85

Table 5
Kinetic parameters for dye adsorption on TSBAC.

Adsorbate	Pseudo-first order			Pseudo-second order			Intraparticle diffusion model		
	q_e (mg/g)	K_1 (min^{-1})	R^2	q_e (mg/g)	K_2 (g/mg.min)	R^2	k_{id} ($mg/g.min^{0.5}$)	C	R^2
MB	65.719	0.036	0.95	116.278	0.002	0.99	8.844	32.553	0.77
RR 198	61.868	0.035	0.91	98.038	0.001	0.98	8.172	17.379	0.83
RY 145	52.247	0.036	0.88	90.908	0.001	0.98	7.704	15.843	0.84
Dyes in Synthetic Textile Effluent	61.706	0.037	0.95	100.000	0.002	0.99	7.826	24.874	0.82

intraparticle diffusion. Film diffusion was reported to be the rate determining step also in case of the adsorption of real textile effluent over alkali-activated sand (Sharma et al., 2019).

3.3. Continuous column adsorption studies

The continuous column adsorption studies were conducted for individual dye solutions along with the synthetic textile effluent. Two dynamic adsorption models namely Adams-Bohart model (Bohart and Adams, 1920) and Thomas model (Thomas, 1944) were applied to model the obtained breakthrough curves. The breakthrough curves at different bed heights obtained for the four adsorbate solutions are presented in Fig. 5. The Adams-Bohart model assumes that the adsorption rate is proportional to residual capacity of the adsorbent and concentration of adsorbate in solution phase (Bohart and Adams, 1920). The Thomas model is applicable when the adsorption process follows Langmuir isotherm with no axial dispersion in the adsorption column (Thomas, 1944). Various dynamic adsorption model parameters for dye adsorption on TSBAC are presented in Table 6. The equations of dynamic adsorption models used in the present study are given in the supplementary material.

As observed from Fig. 5 and Table 6, the breakthrough time (t_b) for all the adsorbate solutions increased with the increase in bed height from 10 to 30 cm. As the bed height increases, a greater number of

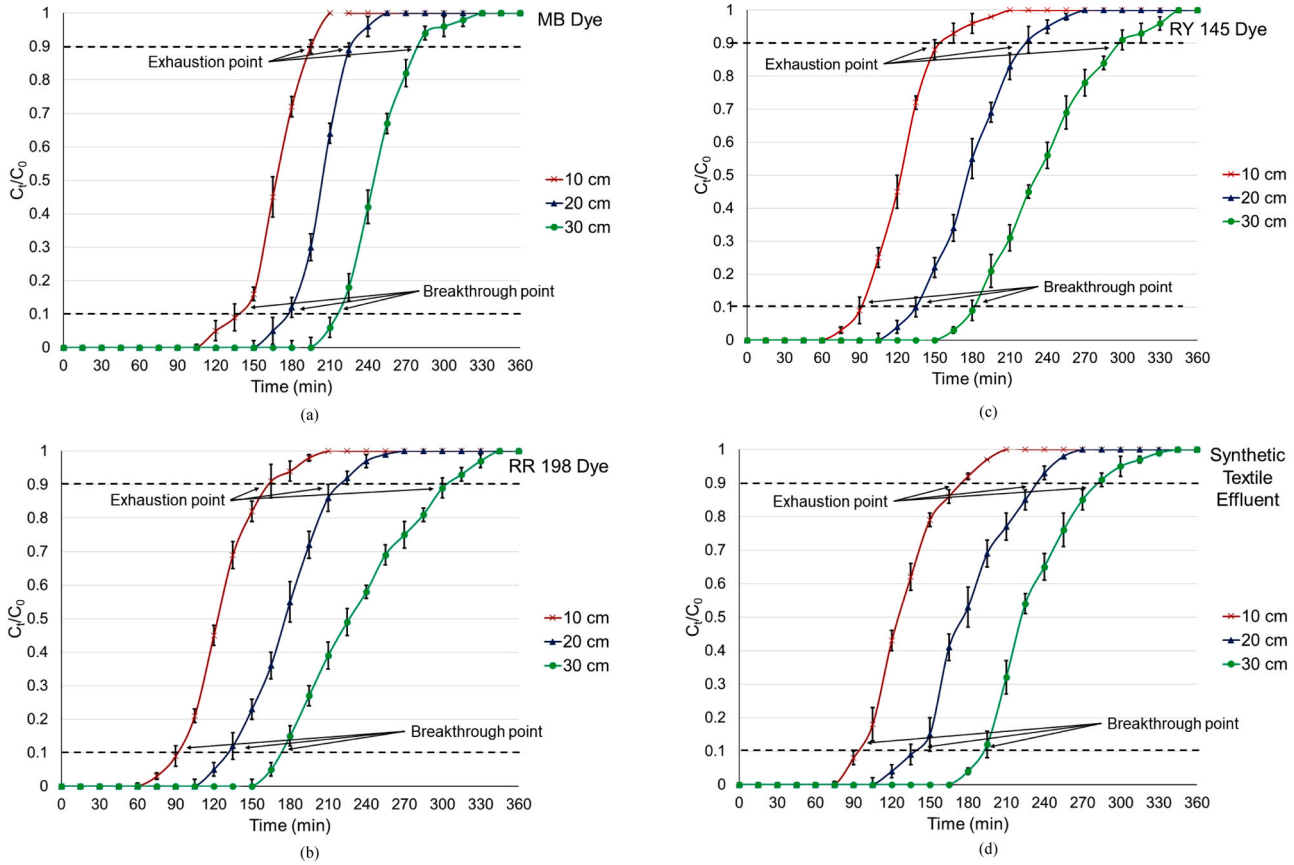

Fig. 5. Breakthrough curves for the adsorption of dyes on TSBAC (Flow rate = 20 mL/min) (a) MB (b) RR 198 (c) RY 145 (d) Synthetic Textile Effluent.

Table 6
Dynamic parameters for dye adsorption on TSBAC.

Adsorbate	Bed height (cm)	$q_{e\ (exp.)}$ (mg/g)	t_b (min)	Adams-Bohart model			Thomas model			Dye removal (%)
				k_{AB} (mL/mg. min)	N_0 (mg/mL)	R^2	k_{TH} (mL/mg. min)	q_0 (mg/g)	R^2	
MB	10	101.8	140	0.16	20.12	0.96	0.27	101.84	0.98	46.4
	20	61.5	177	0.12	15.98	0.92	0.26	61.35	0.99	56.4
	30	49.8	216	0.09	10.71	0.78	0.25	49.95	0.98	68.6
RR 198	10	76.6	93	0.11	17.26	0.81	0.24	77.85	0.99	34.9
	20	53.3	132	0.08	12.10	0.85	0.21	53.03	0.99	48.9
	30	46.9	174	0.06	9.90	0.78	0.13	47.04	0.97	64.7
RY 145	10	75.1	90	0.11	17.05	0.79	0.25	76.24	0.98	34.2
	20	54.1	135	0.08	12.86	0.84	0.20	54.20	0.99	49.5
	30	47.6	183	0.07	10.28	0.77	0.15	48.13	0.98	64.7
Dyes in Synthetic Textile Effluent	10	79.1	96	0.09	17.67	0.81	0.22	79.47	0.99	36.1
	20	54.8	141	0.08	13.26	0.83	0.19	55.06	0.98	50.2
	30	46.6	192	0.07	10.09	0.71	0.18	47.09	0.98	64.2

adsorption sites on the adsorbent will be available for dye removal, resulting to longer breakthrough time. At the 30 cm bed height, optimum adsorption pH, initial dye concentration of 250 mg/L and 20 mL/min flow rate, highest dye removal was obtained for MB (68.6%) as compared to RR 198 (64.7%), RY 145 (64.7%), and dyes from synthetic textile effluent (64.2%), the observation in-line with the findings of batch adsorption studies. Steeper breakthrough curves, earlier attainment of breakthrough point, and exhaustion point was observed for lower adsorbent bed height.

As observed from Table 6, higher R^2 values were obtained for Thomas model (0.97 – 0.99) as compared to Adam-Bohart model (0.71 – 0.96). The predicted q_0 values by Thomas model were in good agreement with the experimental q_e values. The k_{TH} and q_0 values were found to decrease on increasing the bed height for a given adsorbate solution. Similar results were reported by Han et al. (2008) for the adsorption of congo red dye over a 30 cm adsorption column of rice husk. The k_{AB} and N_0 values decreased with increasing bed height for the given adsorbate solution. Similar findings were also reported by López-Cervantes et al. (2018) for azo dye adsorption over a 12 cm column of chitosan-glutaraldehyde biosorbent. For a given adsorbate solution, higher adsorption capacity was found at lower adsorbent bed height as lower bed height caused maximum exploration of adsorbate binding sites. The experimental q_e values for various azo dyes observed in the present study were found to be significantly higher than the q_e values reported by Vasques et al. (2009) for azo dye adsorption by acetic acid activated textile sludge, thus the proposed method of phosphorus acid treatment yielded very good results. The protonated oxygen-containing functional groups on the adsorbent surface will be acting as a binding site for negative sulphonic acid group in the dye structure. The resulting ionic bond formation contributes to higher adsorption capacities of TSBAC.

Packing ratio of the column was calculated as the ratio of volume of packed activated carbon and total volume of the column and was found to be 0.79 (v/v). The HRT was calculated as the ratio of volume of the adsorption column and flow rate. The HRT of the column of bed height 10 cm, 20 cm, and 30 cm was found to be 2.45 min, 4.91 min, and 7.36 min, respectively. A total of 64.2% dye removal was resulted from synthetic textile effluent by the 30 cm adsorption column of TSBAC in presence of higher salt content and other simpler organic compounds presents the field-scale application potential of the developed adsorbent.

3.4. Adsorbent reuse

Based on the adsorbent reuse studies, it was observed that up to six reuse cycles, the reduction in percentage dye removal remained less than 5% of the percentage dye removal by fresh adsorbent. The reduction in dye removal capacity of spent adsorbent during subsequent reuse cycles was attributed to the deposition of sulphate groups from adsorbed dyes over TSBAC surface (Stawiński et al., 2017). The findings suggest, developed adsorbent can be reused up to six reuse cycles without any significant loss in the dye adsorption capacity.

3.5. Leachability studies

The disposal of spent adsorbent after treatment becomes a major concern in case of high desorption potential. The present study ensured that the adsorbed dyes are not desorbed easily from the spent adsorbent after disposal by performing toxicity characteristics leaching procedure (TCLP). Based on the TCLP tests conducted in triplicates, 9%, 7%, and 6% of the adsorbed MB, RR 198, and RY 145, respectively were released from the spent TSBAC.

The extraction solution was also analyzed for heavy metals like lead and chromium as they are used in production of some textile dyes. The concentrations of lead and chromium in extraction solution were found to be well below the detection limit, owing to the gradual phase-out of toxic heavy metal containing dyes by the textile industries.

3.6. Adsorption mechanism

The developed TSBAC presented distinguished adsorption capacity for MB, RR 198, and RY 145 as individual solutions and as synthetic textile effluent. The higher dye adsorption capacity can be ascribed to the presence of oxygen containing functional groups on the surface of TSBAC as demonstrated by FTIR analysis. The nanoporous nature of TSBAC along with high surface area (123.65 m^2/g) facilitates the availability of adsorption sites for dye adsorption even at higher initial dye concentrations.

XPS analysis was performed for the TSBAC before and after adsorption to better understand the adsorption mechanism. The XPS spectra in C1s, O1s, and N1s region were analyzed to understand presence of the active surface function groups on TSBAC as presented in Fig. 6. From Fig. 6(a), peaks at 284.8 eV and 288.3 eV could be assigned to carbon atoms in the binding form of C═C and C═O, respectively (Yang et al., 2015). The peak intensity in C1s region was found to increase in Fig. 6(b) owing to the addition carbon from the adsorbed dye molecules. In Fig. 6(c), for XPS spectra in O1s region the peaks at 533.6 eV and 532 eV indicate the presence of C═O and C−OH, respectively on the surface of TSBAC (Xu et al., 2014). The horizontal shift in the peaks for the spectra obtained after adsorption indicates involvement of C═O and C−OH functional groups in the adsorption mechanism. The XPS spectra in N1s region after adsorption, presents an increase in the intensity of the peak at 399.5 eV corresponding to nitrogen in aromatic rings. The other peak at 393 eV can be attributed to molybdenum, which was used as the base material during XPS analysis. Thus, effective adsorption of the considered dye compounds on TSBAC surface was confirmed from the XPS analysis in N1s region. The

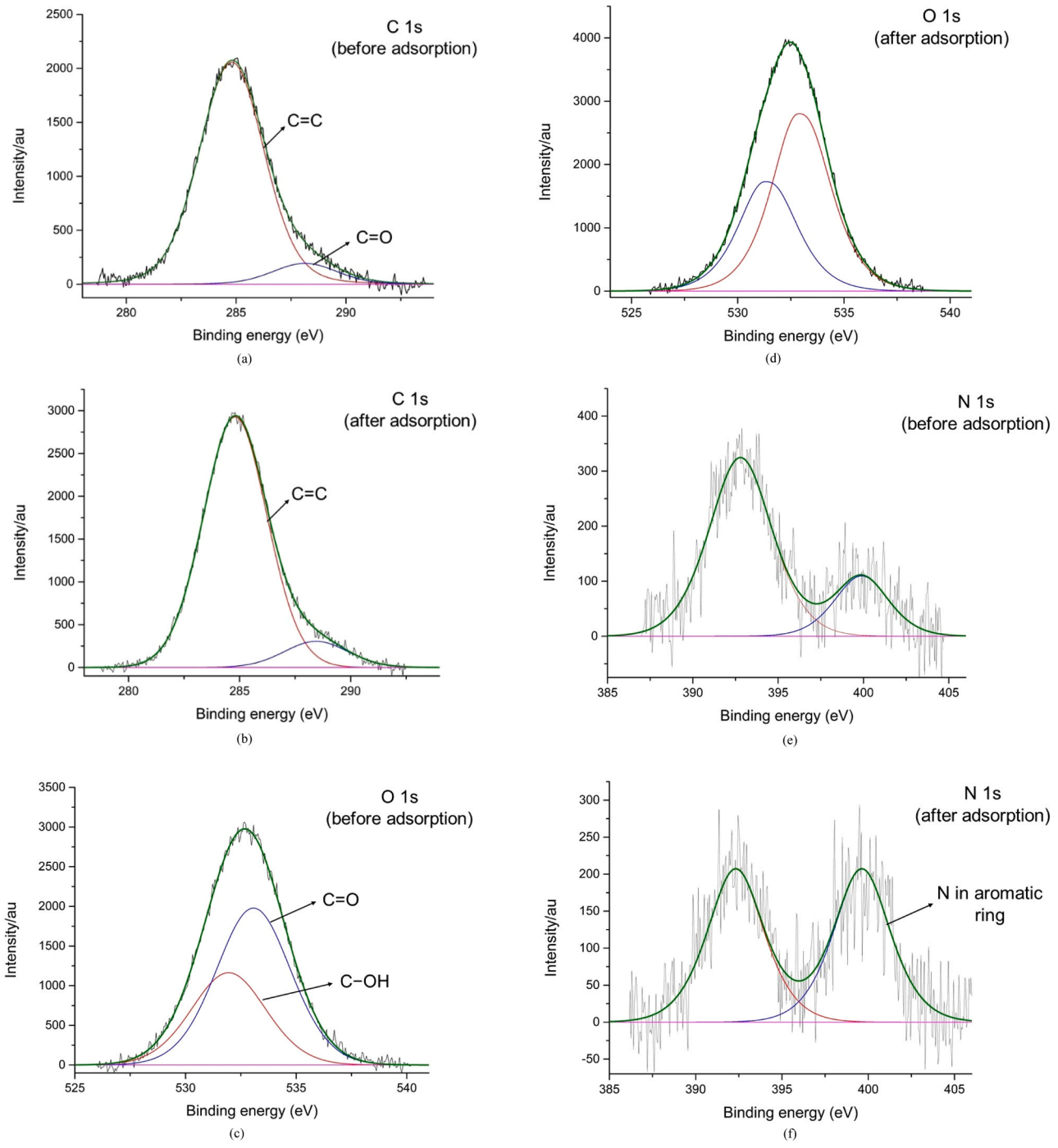

Fig. 6. XPS spectra of C1s, O1s, and N1s region before adsorption (a), (c), (e) and after adsorption (b), (d), (f) for dye adsorption on TSBAC.

plausible mechanism for the adsorptive removal of cationic and anionic dyes by TSBAC estimated based on the adsorbent surface chemistry is presented in Fig. 7. Considering the results of TSBAC surface characterization, adsorption isotherm and kinetics, and column adsorption studies the electrostatic interaction between sulphonic acid group in the hydrolyzed dye molecules and surface functional groups on TSBAC was identified as the major adsorption mechanism along with hydrogen bonding and/or van der Waals interaction. The results of XPS analysis also support the plausible adsorption mechanism presented in Fig. 7. Thus, the developed adsorbent can be efficiently employed to remove both cationic and anionic dyes in the appropriate pH range.

4. Potential Practical Applications and Limitations

Based on the results of continuous column studies, large scale adsorption column of treatment capacity 500 m^3/d was designed. The benchmarking criteria used the scale-up of the design included Empty Bed Contact Time (EBCT) and filtration rate (FR) (Yan et al., 2015; Jung et al., 2017).

The filtration rate for lab-scale adsorption column was found to be 4.07 cm/min, based on which the required diameter for large scale column was calculated as nearly 3.3 m. The amount of TSBAC required for the design treatment capacity of 500 m^3/d was nearly 1550 kg. The breakthrough volume for the design column was obtained as 66.67 m^3.

The presented approach of using textile sludge based adsorbent for

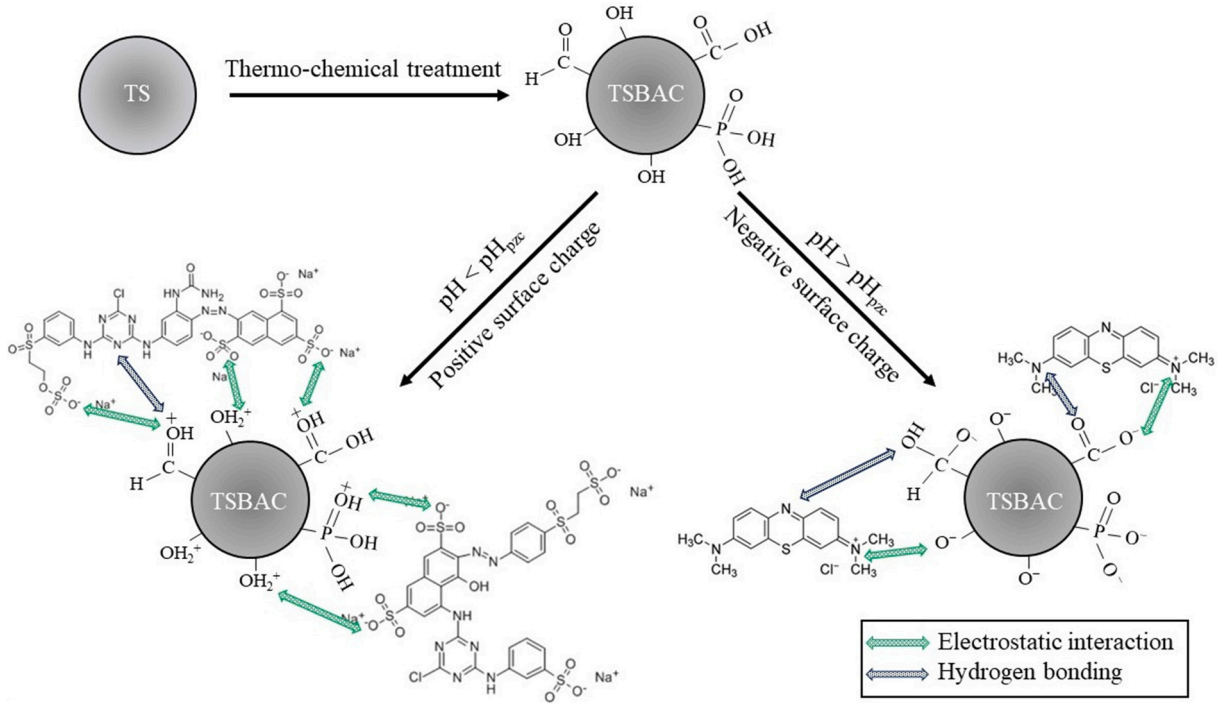

Fig. 7. Plausible mechanism of cationic and anionic dyes adsorption onto TSBAC.

the treatment of textile effluent will provide a win-win situation for major concerns to textile manufacturers regarding management of hazardous textile effluent treatment sludge and color removal from the textile effluent. As the particle size of TSBAC is between 0.1 and 0.4 mm, the adsorbent can be removed from the treated effluent by simple microfiltration. Based on the leachability studies, environmentally sound disposal of the spent adsorbent is possible without any harm to the environment. Some of the limiting factors for field scale application may include textile sludge pretreatment and requirement of acidic pH during treatment. These limitations can be overcome considering the associated benefit of enhanced dye removal resulting in environmental protection, which will compensate the chemical cost involved in pre-treatment and pH adjustment. Some of the previous studies have reported application of the adsorption treatment at a pH range of 2 – 3 including Chakraborty et al. (2006), Ahmad and Hameed (2009).

Table 7
Comparison of dye removal by various sludge-based adsorbents.

Adsorbent type	BET surface area (m^2/g)	Pollutant removed	Adsorption capacity (mg/g)	Reference
Sewage sludge based adsorbent	80	Acid Blue 74 dye	30.8	Otero et al. (2003)
Sewage sludge based adsorbent	61	Acid Yellow 49 dye	116.3	Jindarom et al. (2007)
Textile sludge based adsorbent	44	Reactive Red 2	159.3	Sonai et al. (2016)
Textile sludge based adsorbent	38.4	Reactive Red 141	72.3	Leal et al. (2018)
Textile sludge based adsorbent	123.65	Methylene Blue	123.6	Present study
		Reactive Red 198	101.4	
		Reactive Yellow 145	96.8	

Table 7 presents a comparative performance analysis of the developed TSBAC adsorbent with other previously reported sludge-based adsorbents.

As observed from Table 7, the BET surface area of the developed adsorbent was found to be higher than the BET surface area of the previously reported sludge based adsorbents. The adsorption capacity from individual dye solution, may not reflect the field-scale adsorption capacity from the complex textile effluent matrix. Thus, the reported dye removal of 64.2% from synthetic textile effluent by the 30 cm adsorption column of TSBAC present high practical application potential for the developed adsorbent.

5. Conclusions

The reported study in this paper illustrates a potential technique of value-added waste transformation for the textile effluent treatment sludge along with a beneficial application with-in the industry premises for textile manufacturers. The developed adsorbent presented superior adsorption capacity for methylene blue (123.6 mg/g), reactive red 198 (101.4 mg/g), and reactive yellow 145 (96.8 mg/g) individually, and from the synthetic textile effluent (106 mg/g) within 2 h of batch adsorption. Based on the continuous column adsorption studies, 64.2% dye removal was achieved from the synthetic textile effluent at the flow rate of 20 mL/min by the 30 cm adsorption column of the developed adsorbent owing to the higher specific surface area (123.65 m^2/g) and the presence of active surface functional groups like −OH, −COOH, −C═O on the adsorbent surface. The plausible adsorption mechanism involves the electrostatic interaction between active surface functional groups and sulphonic acid group in the hydrolyzed dye molecules along with hydrogen bonding. The next phase of the research would be to apply the proposed technique for the actual wastewater from textile industries.

CRediT authorship contribution statement

Ninad Oke: Formal analysis, Data curation, Validation, Writing – orignal draft. **S. Mohan:** Methodology, Supervision, Writing – review &

editing, Visualization.

Declaration of Competing Interest

The authors declare that they have no known competing financial interests or personal relationships that could have appeared to influence the work reported in this paper.

Acknowledgements

The authors are thankful to the Sophisticated Analytical Instrumentation Facility (SAIF), IIT Madras for providing necessary facilities for material surface characterization. Authors are also thankful to the NFMTC/MSRC/IITM facility for providing required support to conduct the XPS analysis.

Appendix A. Supporting information

Supplementary data associated with this article can be found in the online version at doi:10.1016/j.jhazmat.2021.126864.

References

Ahmad, A.A., Hameed, B.H., 2009. Reduction of COD and color of dyeing effluent from a cotton textile mill by adsorption onto bamboo-based activated carbon. J. Hazard. Mater. 172 (2–3), 1538–1543. https://doi.org/10.1016/j.jhazmat.2009.08.025.

Basu, M., Guha, A.K., Ray, L., 2019. Adsorption of lead on lentil husk in fixed bed column bioreactor. Bioresour. Technol. 283, 86–95. https://doi.org/10.1016/j.biortech.2019.02.133.

Begum, B.S.S., Gandhimathi, R., Ramesh, S.T., Nidheesh, P.V., 2013. Utilization of textile effluent wastewater treatment plant sludge as brick material. J. Mater. Cycles Waste Manag. 15, 564–570. https://doi.org/10.1007/s10163-013-0139-4.

Beshah, D.A., Tiruye, G.A., Mekonnen, Y.S., 2021. Characterization and recycling of textile sludge for energy-efficient brick production in Ethiopia. Environ. Sci. Pollut. Res. 28, 16272–16281. https://doi.org/10.1007/s11356-020-11878-7.

Blanchard, G., Maunaye, M., Martin, G., 1984. Removal of heavy metals from waters by means of natural zeolites. Water Res 18 (12), 1501–1507.

Bohart, G., Adams, E.Q., 1920. Some aspects of the behaviour of charcoal with respect to chlorine. J. Am. Chem. Soc. 42, 523–544.

Chakraborty, S., Basu, J.K., De, S., DasGupta, S., 2006. Adsorption of reactive dyes from a textile effluent using sawdust as the adsorbent. In: Ind. Eng. Chem. Res, 45, pp. 4732–4741. https://doi.org/10.1021/ie050302f CCC.

Cheng, J., Gu, J.J., Tao, W., Wang, P., Liu, L., Wang, C.Y., Li, Y.K., Feng, X.H., Qiu, G.H., Cao, F.F., 2019. Edible fungus slag derived nitrogen-doped hierarchical porous carbon as a high-performance adsorbent for rapid removal of organic pollutants from water. Bioresour. Technol. 294, 122149 https://doi.org/10.1016/j.biortech.2019.122149.

Choudhary, M., Kumar, R., Neogi, S., 2020. Activated biochar derived from Opuntia ficus-indica for the efficient adsorption of malachite green dye, Cu+2 and Ni+2 from water. J. Hazard. Mater. 392, 122441 https://doi.org/10.1016/j.jhazmat.2020.122441.

Freundlich, H., 1909. Kapillarchemie: Eine Darstellung der Chemie der Kolloide und verwandter Gebiete. Akademische Verlagsgesellschaf, Leipzig, Germany.

Giles, C.H., Smith, D., Huiston, A., 1974. A general treatment and classification of the solute adsorption isotherms. J. Colloid Interface Sci. 47, 755–765.

Gopi, S., Pius, A., Kargl, R., Kleinschek, K.S., Thomas, S., 2019. Fabrication of cellulose acetate/chitosan blend films as efficient adsorbent for anionic water pollutants. Polym. Bull. 76 (3), 1557–1571. https://doi.org/10.1007/s00289-018-2467-y.

Gupta, A., Garg, A., 2015. Utilisation of sewage sludge derived adsorbents for the removal of recalcitrant compounds from wastewater: mechanistic aspects, isotherms, kinetics and thermodynamics. Bioresour. Technol. 194, 214–224. https://doi.org/10.1016/j.biortech.2015.07.005.

Haider, S., Bukhari, N., Park, S.Y., Iqbal, Y., Al-Masry, W.A., 2011. Adsorption of bromophenol blue from an aqueous solution onto thermally modified granular charcoal. Chem. Eng. Res. Des. 89 (1), 23–28. https://doi.org/10.1016/j.cherd.2010.04.022.

Han, R., Ding, D., Xu, Y., Zou, W., Wang, Y., Li, Y., Zou, L., 2008. Use of rice husk for the adsorption of congo red from aqueous solution in column mode. Bioresour. Technol. 99, 2938–2946. https://doi.org/10.1016/j.biortech.2007.06.027.

Haque, N., 2020. Mapping prospects and challenges of managing sludge from effluent treatment in Bangladesh. J. Clean. Prod. 259, 120898 https://doi.org/10.1016/j.jclepro.2020.120898.

Jiang, C., Wang, X., Qin, D., Da, W., Hou, B., Hao, C., Wu, J., 2019. Construction of magnetic lignin-based adsorbent and its adsorption properties for dyes. J. Hazard. Mater. 369, 50–61. https://doi.org/10.1016/j.jhazmat.2019.02.021.

Jindarom, C., Meeyoo, V., Kitiyanan, B., Rirksomboon, T., Rangsunvigit, P., 2007. Surface characterization and dye adsorptive capacities of char obtained from pyrolysis/gasification of sewage sludge. Chem. Eng. J. 133 (1–3), 239–246. https://doi.org/10.1016/j.cej.2007.02.002.

Jung, K.W., Jeong, T.U., Choi, J.W., Ahn, K.H., Lee, S.H., 2017. Adsorption of phosphate from aqueous solution using electrochemically modified biochar calcium-alginate beads: batch and fixed-bed column performance. Bioresour. Technol. 244, 23–32. https://doi.org/10.1016/j.biortech.2017.07.133.

Khan, A.Y., Kumar, G.S., 2016. Spectroscopic studies on the binding interaction of phenothiazinium dyes, azure A and azure B to double stranded RNA polynucleotides. Spectrochim. Acta Part A Mol. Biomol. Spectrosc. 152, 417–425. https://doi.org/10.1016/j.saa.2015.07.091.

Kołodyńska, D., Gęca, M., Pylypchuk, I.V., Hubicki, Z., 2016. Development of new effective sorbents based on nanomagnetite. Nanoscale Res. Let. 11 (1), 1–10. https://doi.org/10.1186/s11671-016-1371-3.

Kusworo, T.D., Aryanti, N., Utomo, D.P., 2018. Oilfield produced water treatment to clean water using integrated activated carbon-bentonite adsorbent and double stages membrane process. Chem. Eng. J. 347, 462–471. https://doi.org/10.1016/j.cej.2018.04.136.

Lagergren, S.K., 1898. About the theory of so-called adsorption of soluble substances, 24. Sven. Vetenskapsakad. Handl., pp. 1–39

Langmuir, I., 1916. The constitution and fundamental properties of solids and liquids. Part I. Solids. J. Am. Chem. Soc. 38 (11), 2221–2295. https://doi.org/10.1021/Ja02268a002.

Leal, T.W., Lourenco, L.A., Scheibe, A.S., de Souza, S.M.G.U., de Souza, A.A.U., 2018. Textile wastewater treatment using low-cost adsorbent aiming the water reuse in dyeing process. J. Environ. Chem. Eng. 6, 2705–2712. https://doi.org/10.1016/j.jece.2018.04.008.

Lei, J., Liu, H., Yuan, C., Chen, Q., Liu, J.A., Wen, F., Jiang, X., Deng, W., Cui, X., Duan, T., Zhu, W., He, R., 2021a. Enhanced photoreduction of U (VI) on WO3 nanosheets by oxygen defect engineering. Chem. Eng. J. 416, 129164 https://doi.org/10.1016/j.cej.2021.129164.

Lei, J., Liu, H., Wen, F., Jiang, X., Yuan, C., Chen, Q., Liu, J., Cui, X., Yang, F., Zhu, W., He, R., 2021b. Tellurium nanowires wrapped by surface oxidized tin disulfide nanosheets achieves efficient photocatalytic reduction of U (VI). Chem. Eng. J. 426, 130756 https://doi.org/10.1016/j.cej.2021.130756.

Lellis, B., Fávaro-Polonio, C.Z., Pamphile, J.A., Polonio, J.C., 2019. Effects of textile dyes on health and the environment and bioremediation potential of living organisms. Biotechnol. Res. Innov. 3 (2), 275–290. https://doi.org/10.1016/j.biori.2019.09.001.

Liu, Q., Li, Y., Chen, H., Lu, J., Yu, G., Möslang, M., Zhou, Y., 2020. Superior adsorption capacity of functionalised straw adsorbent for dyes and heavy-metal ions. J. Hazard. Mater. 382, 121040 https://doi.org/10.1016/j.jhazmat.2019.121040.

Liu, H., Lei, J., Yang, S., Qin, F., Cui, L., Kong, Y., Zheng, X., Duan, T., Zhu, W., He, R., 2021. Boosting the oxygen evolution activity over cobalt nitride nanosheets through optimizing the electronic configuration. Appl. Catal. B Environ. 286, 119894 https://doi.org/10.1016/j.apcatb.2021.119894.

López-Cervantes, J., Sánchez-Machado, D.I., Sánchez-Duarte, R.G., Correa-Murrieta, M. A., 2018. Study of a fixed-bed column in the adsorption of an azo dye from an aqueous medium using a chitosan–glutaraldehyde biosorbent. Adsorpt. Sci. Technol. 36 (1–2), 215–232. https://doi.org/10.1177/0263617416688021.

Mahmoud, D.K., Salleh, M.A., Karim, W.A., Idris, A., Abidin, Z.Z., 2012. Batch adsorption of basic dye using acid treated kenaf fibre char: equilibrium, kinetic and thermodynamic studies. Chem. Eng. J. 181, 449–457. https://doi.org/10.1016/j.cej.2011.11.116.

Mamaní, A., Ramírez, N., Deiana, C., Giménez, M., Sardella, F., 2019. Highly microporous sorbents from lignocellulosic biomass: Different activation routes and their application to dyes adsorption. J. Environ. Chem. Eng. 7, 103148 https://doi.org/10.1016/j.jece.2019.103148.

Mohan, S., Gandhimathi, R., 2009. Removal of heavy metal ions from municipal solid waste leachate using coal fly ash as an adsorbent. J. Hazard. Mater. 169, 351–359. https://doi.org/10.1016/j.jhazmat.2009.03.104.

Mohan, S., Sreelakshmi, G., 2008. Fixed bed column study for heavy metal removal using phosphate treated rice husk. J. Hazard. Mater. 153, 75–82. https://doi.org/10.1016/j.jhazmat.2007.08.021.

Otero, M., Rozada, F., Calvo, L.F., Garcia, A.I., Moran, A., 2003. Elimination of organic water pollutants using adsorbents obtained from sewage sludge. Dyes Pigments 57 (1), 55–65. https://doi.org/10.1016/S0143-7208(03)00005-6.

Oyekanmi, A.A., Ahmad, A., Hossain, K., Rafatullah, M., 2019. Adsorption of Rhodamine B dye from aqueous solution onto acid treated banana peel: response surface methodology, kinetics and isotherm studies. PLoS ONE 14 (5), 0216878. https://doi.org/10.1371/journal.pone.0216878.

Patel, H., Vashi, R.T., 2010. Treatment of textile wastewater by adsorption and coagulation. E-J. Chem. 7 (4), 1468–1476.

Paździor, K., Bilińska, L., Ledakowicz, S., 2017. Influence of ozonation and biodegradation on toxicity of industrial textile wastewater. J. Environ. Manag. 195, 166–173. https://doi.org/10.1016/j.cej.2018.12.057.

Rahman, M.M., Khan, M.M.R., Uddin, M.T., Islam, M.A., 2017. Textile effluent treatment plant sludge: characterization and utilization in building materials. Arab. J. Sci. Eng. 42, 1435–1442. https://doi.org/10.1007/s13369-016-2298-9.

Reffas, A., Bernardet, V., David, B., Reinert, L., Lehocine, M.B., Dubois, M., Batisse, N., Duclaux, L., 2010. Carbons prepared from coffee grounds by H3PO4 activation: characterization and adsorption of methylene blue and Nylosan Red N-2RBL. J. Hazard. Mater. 175, 779–788. https://doi.org/10.1016/j.jhazmat.2009.10.076.

Saha, P.D., Chakraborty, S., Chowdhury, S., 2012. Batch and continuous (fixed-bed column) biosorption of crystal violet by Artocarpus heterophyllus (jackfruit) leaf powder. Colloids Surf. B Biointerfaces 92, 262–270. https://doi.org/10.1016/j.colsurfb.2011.11.057.

Saheed, I.O., Adekola, F.A., Olatunji, G.A., 2017. Sorption study of methylene blue on activated carbon prepared from Jatropha curcas and Terminalia catappa seed coats.

J. Turk. Chem. Soc. Sect. A Chem. 4 (1), 375–394. https://doi.org/10.18596/jotcsa.287337.

Sharma, A., Syed, Z., Brighu, U., Gupta, A.B., Ram, C., 2019. Adsorption of textile wastewater on alkali-activated sand. J. Clean. Prod. 220, 23–32. https://doi.org/10.1016/j.jclepro.2019.01.236.

Sonai, G.G., de Souza, S.M.G.U., de Oliveira, D., de Souza, A.A.U., 2016. The application of textile sludge adsorbents for the removal of Reactive Red 2 dye. J. Environ. Manag. 168, 149–156. https://doi.org/10.1016/j.jenvman.2015.12.003.

Spagnoli, A.A., Giannakoudakis, D.A., Bashkova, S., 2017. Adsorption of methylene blue on cashew nut shell based carbons activated with zinc chloride: the role of surface and structural parameters. J. Mol. Liq. 229, 465–471. https://doi.org/10.1016/j.molliq.2016.12.106.

Stawiński, W., Węgrzyn, A., Freitas, O., Chmielarz, L., Figueiredo, S., 2017. Dual-function hydrotalcite-derived adsorbents with sulfur storage properties: dyes and hydrotalcite fate in adsorption-regeneration cycles. Micro Mesoporous Mater. 250, 72–87. https://doi.org/10.1016/j.micromeso.2017.05.017.

Tang, Y., Zhao, Y., Lin, T., Li, Y., Zhou, R., Peng, Y., 2019. Adsorption performance and mechanism of methylene blue by H3PO4-modified corn stalks. J. Environ. Chem. Eng. 7, 103398 https://doi.org/10.1016/j.jece.2019.103398.

Temkin, M.J., Pyzhev, V., 1940. Recent modifications to Langmuir isotherms. Acta Phys. - Chim. Sin. 12, 217–222.

Thomas, H.C., 1944. Heterogeneous ion exchange in a flowing system. J. Am. Chem. Soc. 66, 1664–1666.

U.S. EPA, 2012. Test Methods for Evaluating Solid Waste, Physical/Chemical Methods, SW-846, 3rd ed. U.S. Government Printing Office, Washington, DC.

Varjani, S., Rakholiya, P., Ng, H.Y., You, S., Teixeira, J.A., 2020. Microbial degradation of dyes: an overview. Bioresour. Technol. 314, 123728 https://doi.org/10.1016/j.biortech.2020.123728.

Vasques, A.R., de Souza, S.M.G.U., Valle, J.A., Ulson de Souza, A.A., 2009. Application of ecological adsorbent in the removal of reactive dyes from textile effluents. J. Chem. Technol. Biotechnol. 84, 1146–1155. https://doi.org/10.1002/jctb.2147.

Venkataraghavan, R., Thiruchelvi, R., Sharmila, D., 2020. Statistical optimization of textile dye effluent adsorption by Gracilaria edulis using Plackett-Burman design and response surface methodology. Heliyon 6 (10), 05219. https://doi.org/10.1016/j.heliyon.2020.e05219.

Weber Jr., W.J., Morris, J.C., 1963. Kinetics of adsorption on carbon from solution. J. Sanit. Eng. Div. 89 (2), 31–59.

Wong, S., Ngadi, N., Inuwa, I.M., Hassan, O., 2018. Recent advances in applications of activated carbon from biowaste for wastewater treatment: a short review. J. Clean. Prod. 175, 361–375. https://doi.org/10.1016/j.jclepro.2017.12.059.

Wu, J., Yang, J., Feng, P., Huang, G., Xu, C., Lin, B., 2020. High-efficiency removal of dyes from wastewater by fully recycling litchi peel biochar. Chemosphere 246, 125734. https://doi.org/10.1016/j.chemosphere.2019.125734.

Wu, Q.Y., Liang, H.Q., Li, M., Liu, B.T., Xu, Z.K., 2016. Hierarchically porous carbon membranes derived from PAN and their selective adsorption of organic dyes. Chin. J. Polym. Sci. 34 (1), 23–33. https://doi.org/10.1007/s10118-016-1723-6.

Xu, J., Chen, L., Qu, H., Jiao, Y., Xie, J., Xing, G., 2014. Preparation and characterization of activated carbon from reedy grass leaves by chemical activation with H3PO4. Appl. Surf. Sci. 320, 674–680. https://doi.org/10.1016/j.apsusc.2014.08.178.

Yadav, S., Asthana, A., Singh, A.K., Chakraborty, R., Vidya, S.S., Susan, M.A.B.H., Carabineiro, S.A., 2021. Adsorption of cationic dyes, drugs and metal from aqueous solutions using a polymer composite of magnetic/β-cyclodextrin/activated charcoal/Na alginate: isotherm, kinetics and regeneration studies. J. Hazard. Mater. 409, 124840 https://doi.org/10.1016/j.jhazmat.2020.124840.

Yan, L., Huang, Y., Cui, J., Jing, C., 2015. Simultaneous As(III) and Cd removal from copper smelting wastewater using granular TiO2 columns. Water Res 68, 572–579.

Yang, X., Shi, Z., Liu, L., 2015. Adsorption of Sb (III) from aqueous solution by QFGO particles in batch and fixed-bed systems. Chem. Eng. J. 260, 444–453. https://doi.org/10.1016/j.cej.2014.09.036.

Yao, X., Ji, L., Guo, J., Ge, S., Lu, W., Chen, Y., Cai, L., Wang, Y., Song, W., 2020. An abundant porous biochar material derived from wakame (Undaria pinnatifida) with high adsorption performance for three organic dyes. Bioresour. Technol. 318, 124082 https://doi.org/10.1016/j.biortech.2020.124082.

Zhan, B.J., Li, J.S., Xuan, D.X., Poon, C.S., 2020. Recycling hazardous textile effluent sludge in cement-based construction materials: physicochemical interactions between sludge and cement. J. Hazard. Mater. 381, 121034 https://doi.org/10.1016/j.jhazmat.2019.121034.

Zheng, X., Zhou, Y., Liu, X., Fu, X., Peng, H., Lv, S., 2020. Enhanced adsorption capacity of MgO/N-doped active carbon derived from sugarcane bagasse. Bioresour. Technol. 297, 122413 https://doi.org/10.1016/j.biortech.2019.122413.